MATERIALS USED IN MICROPILES IN JAPAN

Mr. Shimazu, Japanese Association for Steel Pipe Piles, Japan

Experimental Study On Ultimate Behavior Of Steel Pipe Pile Group

Masataka Tatsuta[1], Yukitake Shioi[2], Makoto Kimura[3], Akiomi Shimazu[4], Ei Yoshida[5], Kimitoshi Takano[5]

ABSTRACT

Lateral loading model tests are carried out on steel pipe pile group. Each model is composed of four steel pipes (diameter ; 216.3mm, thickness ; 4.5mm) with the different length of filled concrete at the both ends of the steel pipes. From the experimental results, it is found that the horizontal load increases until the buckling occurs at the all ends of steel pipes and that, with more than the concrete filled length of 1D (D : diameter of pipe), the ductility of the steel pipe pile group after the occurrence of inelastic buckling is extremely improved.

INTRODUCTION

In Japan, earthquake load is a dominant factor in the foundation design. So steel pipe piles have been widely used for foundation.

Foundation have been designed based on the allowable stress method. However after Southern Hyogo Prefectual Earthquake, the limit state design will be adopted to the bridge foundation design. As the limit state for pile foundation, we must consider the limit state of bearing capacity, lateral resistance of soil and the pipe structure. We conducted the pipe pile

[1] Japanese Association for Steel Pipe Piles

[2] Professor, Hachinohe University

[3] Assistant Professor, Kyoto University

[4] Executive Director, Japanese Association for Steel Pipe Piles

[5] Japanese Association for Steel Pipe Piles

group model test , in order to clarify the limit state of pipe pile group as structure itself and the effect of the filled concrete filled in the pile top, which improve the ductility of steel pile group.

OUTLINE OF EXPERIMENT

SPECIMENS

The pipe pile group model is shown in Fig.1. The each model had four steel pipes between two concrete footings. The pipes are 216.3mm in diameter, 4.5mm in thickness, and are made of SKK400(nominal tensile strength is 400 MPa). The pipes are put into the concrete footings in the length of 1.5D, where D is the diameter of the pipes.
The tests employed four types of models as shown in Fig. CASE1 was not filled concrete inside the pipes. CASE2 was filled concrete fully inside the pipes. CASE 3 was filled concrete with the length of 1D in the end of the pipes and CASE4 was filled concrete 3D in the pipes.

LOADING METHOD

The test configuration are shown in Fig.3. In the experiments, the axial force (=60 tf) was first applied the vertical center-hole jack to the specimen. With the axial force kept constant, the specified cyclic horizontal load was quasi-statically applied by the horizontal hydraulic jack at the loading point of the center of the upper concrete footing.

The loading program is schematically shown in Fig.4, where δ_y is the displacement of the loading point when the pipe yields at the lower end (right above the lower footing). The specimen was first alternately loaded with the half amplitude of δ_y and alternately loaded by gradually increasing the amplitude of δ_y as the integral multiples of the displacement δ_y like $\pm 2\,\delta_y$, $\pm 3\,\delta_y$, $\pm 5\,\delta_y$, $\pm 10\,\delta_y$, $\pm 15\,\delta_y$. After the cycle of $\pm 15\,\delta_y$, the specimen loaded one direction until it developed 250mm of the lateral displacement or its lateral force dropped below its yield lateral load. In the experiments work, each cyclic load was applied for 3 cycle at the each level of δ_y. The basic displacement δ_y under cyclic loading is calculated using σ_y, which is the yield stress of

steel and is 2400 kgf/cm^2 (nominal yield point of SKK400).

EXPERIMENTS RESULTS

LOAD-DISPLACEMENT RELATIONS AND FRACTURE PROCESS

The horizontal load - horizontal displacement relations are shown in Fig.5 and the horizontal load - vertical displacement relations are shown in Fig.6. Photo.1 shows the pipe pile group model under test.

CASE 1

The horizontal load increased until $\pm 8\ \delta y$ and did not reduced in the cyclic loading at the same amplitude. In $\pm 8\ \delta y$ cycle, inelastic buckling at the lower end of the pipe at the compressive side was observed , but when loaded reverse, local buckling was not observed.
In the cyclic loading at $\pm 10\ \delta y$, the horizontal load decreased a little compared with previous cycle , and in the cyclic loading at same amplitude, the horizontal load decreased. At this cycle, the vertical displacement increased and local buckling at the end of the pipe remained when it loaded reverse. In the cyclic loading at $\pm 15\ \delta y$, the horizontal load of the first cycle dropped to about 80% of the maximum horizontal load and the horizontal load of the third cycle dropped to half of the first cycle load at the same amplitude. After this cycle, the specimen loaded until it developed 170mm of the horizontal displacement and the horizontal load was not lager than half of the maximum horizontal load. Finally the inelastic buckling progressed, resulting into what is called the elephant buckling mode as shown in Photo.2.

CASE 2

The horizontal load increased until $\pm 15\ \delta y$ and didn't reduced so much in the cyclic loading at the same amplitude. After $\pm 15\ \delta y$ cycle, the specimen loaded until it developed 250mm of the horizontal displacement and the horizontal load increased slowly. CASE2 had the larger load carrying capacity and stiffness compared with CASE1.

CASE3

CASE3 recorded the almost same load-displacements relations as CASE1 until the horizontal load exceeded the maximum load. In the cyclic loading at ±15 δ y, the horizontal load of the first cycle dropped to about 80% of the maximum horizontal load as same as CASE1 but the horizontal load of the third cycle dropped to 80% of the first cycle load. Photo.3(a) and (b) show the deformation of the pipe at 8 δ y and at 15 δ y, respectively. After this cycle, the specimen loaded until it developed 250mm of the horizontal displacement and the horizontal load gradually increased to the load of the first cycle at ±15 δ y. The effect of the filled concrete appeared only after maximum loads exceeded and inelastic buckling occurred.

CASE4

CASE4 recorded the similar load-displacements relations to CASE3. But CASE4 had the larger load carrying capacity and stiffness compared with CASE3 and the maximum horizontal load is 15% larger than that of CASE1 and CASE3.

LOAD CARRYING CAPACITY

The maximum horizontal load measured in the experiments are listed in Table 1. CASE2, with filled concrete in the pipes, had the largest load carrying capacity and the load carrying capacity is about 50% larger than that of CASE1. CASE3, with 1D filled concrete at the end of the pipes, had the same load carrying capacities as CASE1. CASE4, with 3D filled concrete at the end of the pipes, had the about15% larger load carrying capacity than CASE1 had. Fully filled concrete made the load carrying capacity large but the effect of filled concrete with the length of 1D and 3D didn't appeared so much in the load carrying capacity.

The calculated interaction relationships among Msp, Msy, Mcsp and N for the pipes are shown in Fig.7, where Msp is the fully plastic moment of the steel pipe and Msy is the yield moment of the steel pipe ; and Mcsp is the fully plastic moment of the steel and concrete composite pipe ; and N is the axial force. The calculated interaction relations among M and N of the each pipes of the pipe group model are also shown in Fig.7.

The horizontal load at which the moment of the pipe equals to the fully plastic moment are listed Table2. The load carrying capacity of CASE1 was close to the load at which the moments of PILE2,3,4 exceed Msp. The load carrying capacity of CASE2 was close to the load at which the moment of PILE 1 exceed Mcsp. It is found that the horizontal load doesn't drop until all pipe exceed the fully plastic moment.

THE DEFORMATION CAPACITY

The envelopes of the horizontal load-horizontal displacement relations are shown in Fig.8. CASE3 and CASE1 were almost the same before the maximum loading point. But after the maximum loading point, the deformation capacity of CASE3 was greatly improved compared with that of CASE1. CASE3 and CASE4 maintained more than 80% of the maximum load at the maximum displacement in the experiments and showed the good deformation capacity. The test results showed that more than 1D filled concrete at the end of the pipes greatly improve the deformation capacity.

Photo.4 shows the filled concrete after the experiments. CASE2, CASE3 and CASE4 had the large crack at the end if the pipes. In CASE2 filled concrete wasn't damaged. In CASE3 the filled concrete had one large transverse crack and in CASE4 the filled concrete had some thin transverse cracks.

FINITE ELEMENT ANALYSIS

The analysis was performed on a single pipe (with 600 mm in diameter and with 9 mm in thickness) by means of FEM aiming at clarifying the effect of the filled concrete at the end of pipe. Two types of models were analyzed, one is without filled concrete ; CASE-A, the other is with 1D filled concrete; CASE-B.

The results of experiments shows that the filled concrete effected on the behavior of the pipe group after inelastic buckling occurred. So the models were given the same deformation as the inelastic buckling deformation at the end of the pipe shown in Fig.9. The two height of the deformation (δ_B) were employed, 10mm(CASE-10A and CASE-10B) and

20mm(CASE-10B and CASE-20B). The joint element function was used between steel pipe and concrete . The function set to no tensile strength and 0.65 in friction coefficient between steel and concrete.

The horizontal load - displacements relations are shown in Fig.10. The results shows that the horizontal load of CASE-B is larger than that of CASE-A in the same deformation and that as the deformation are larger, the effect of filled concrete are larger.

Fig.11 shows the distribution of the axial stress of the pipe of CASE - 20A and CASE-20B at the displacement of 50mm. The compression zone of CASE-20A is larger than that of CASE-20B. The deformation by inelastic buckling makes more reduce compressive rigidity than tensile one. But in CASE-B filled concrete carries compressive stress.

Fig .12 shows the contact point between steel and concrete and Fig.13 shows stress distribution of the filled concrete in CASE -20B. The pipe deformed outside at the top of the inelastic bucking , but deformed inside above the inelastic bucking. The compressive stress transferred from the steel pipe to the concrete mainly just above the inelastic buckling.

CONCLUSION

1) The horizontal load increases until all pipe exceed the fully plastic moment and inelastic buckling occurs at the all ends of steel pipes .

2) Fully filled concrete in the pipes makes the load carrying capacity large but the effect of the filled concrete with the length of 1D or 3D dose not appeared so much in the load carrying capacity.

3) With more than the concrete filled length of 1D (D : diameter of pipe), the ductility of the steel pipe pile group after the occurrence of inelastic buckling is extremely improved.

4) In case of the concrete filled length of 1D, after the occurrence of inelastic buckling, the compressive stress transferred from the steel pipe to the concrete mainly just above the inelastic buckling deformation.

ACKNOWLEDGMENTS

The authors are grateful to the students of Hachinohe Institute of Technology and Kyoto University ,who performed the experiments.

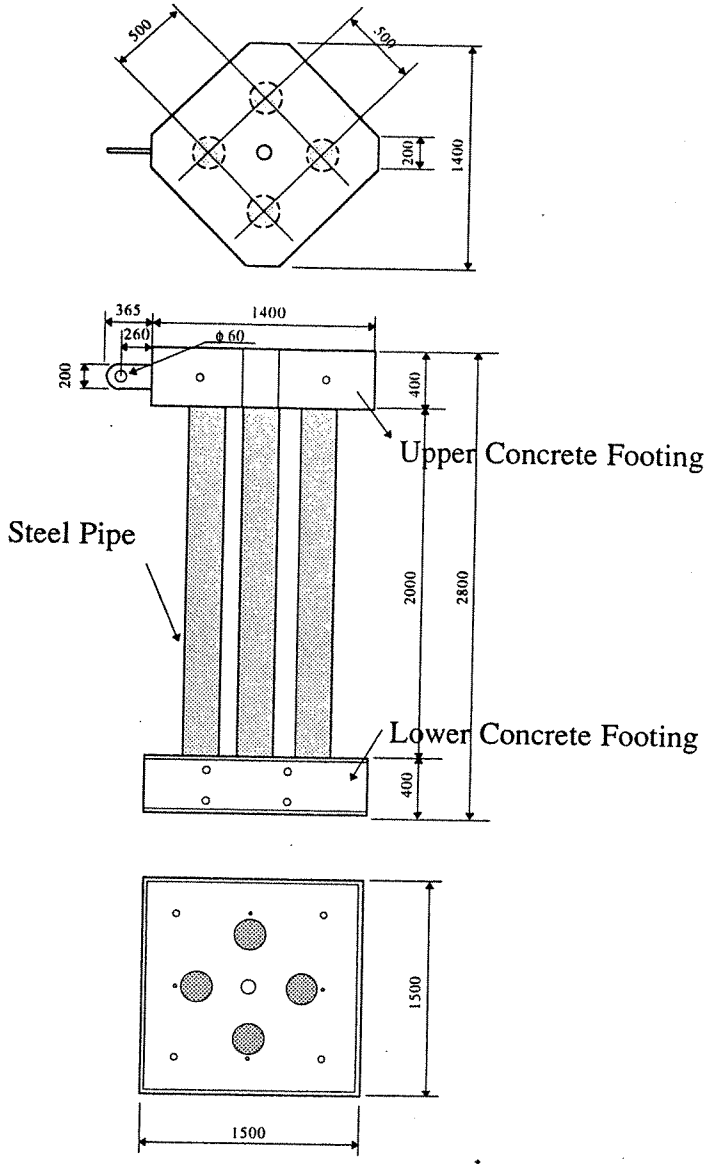

Fig. 1 Test Specimen

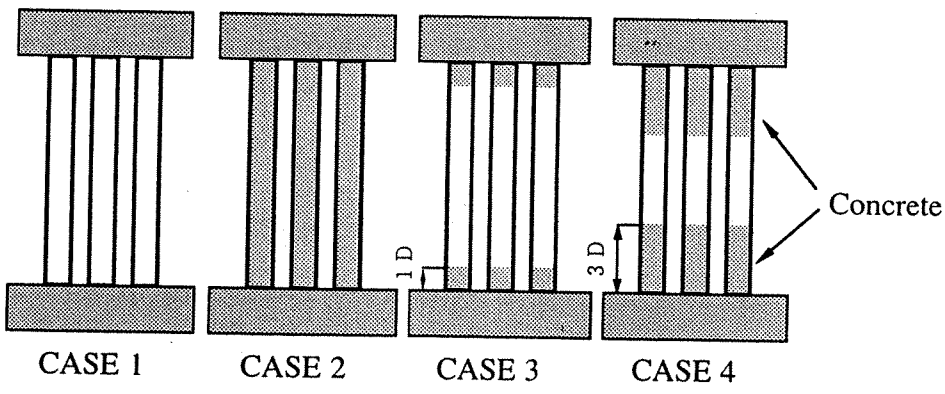

Fig. 2 Four Types of Model

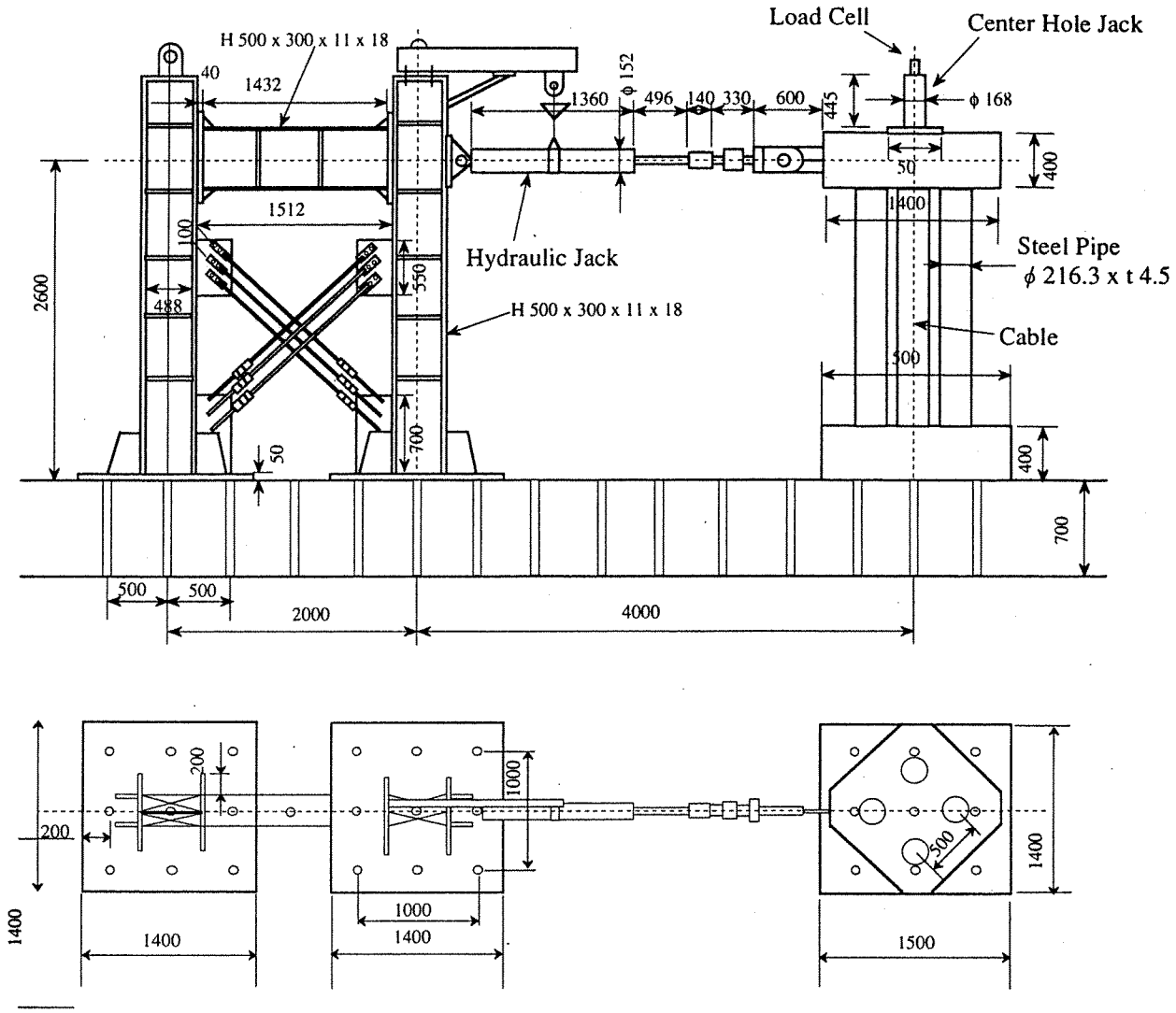

Fig.3 Test Setup

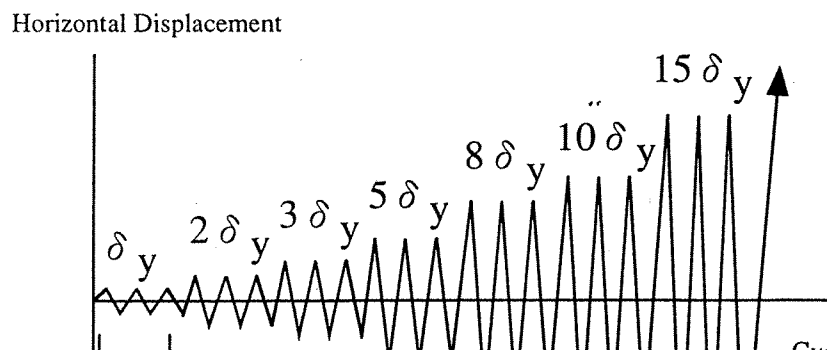

Fig.4 Loading Program

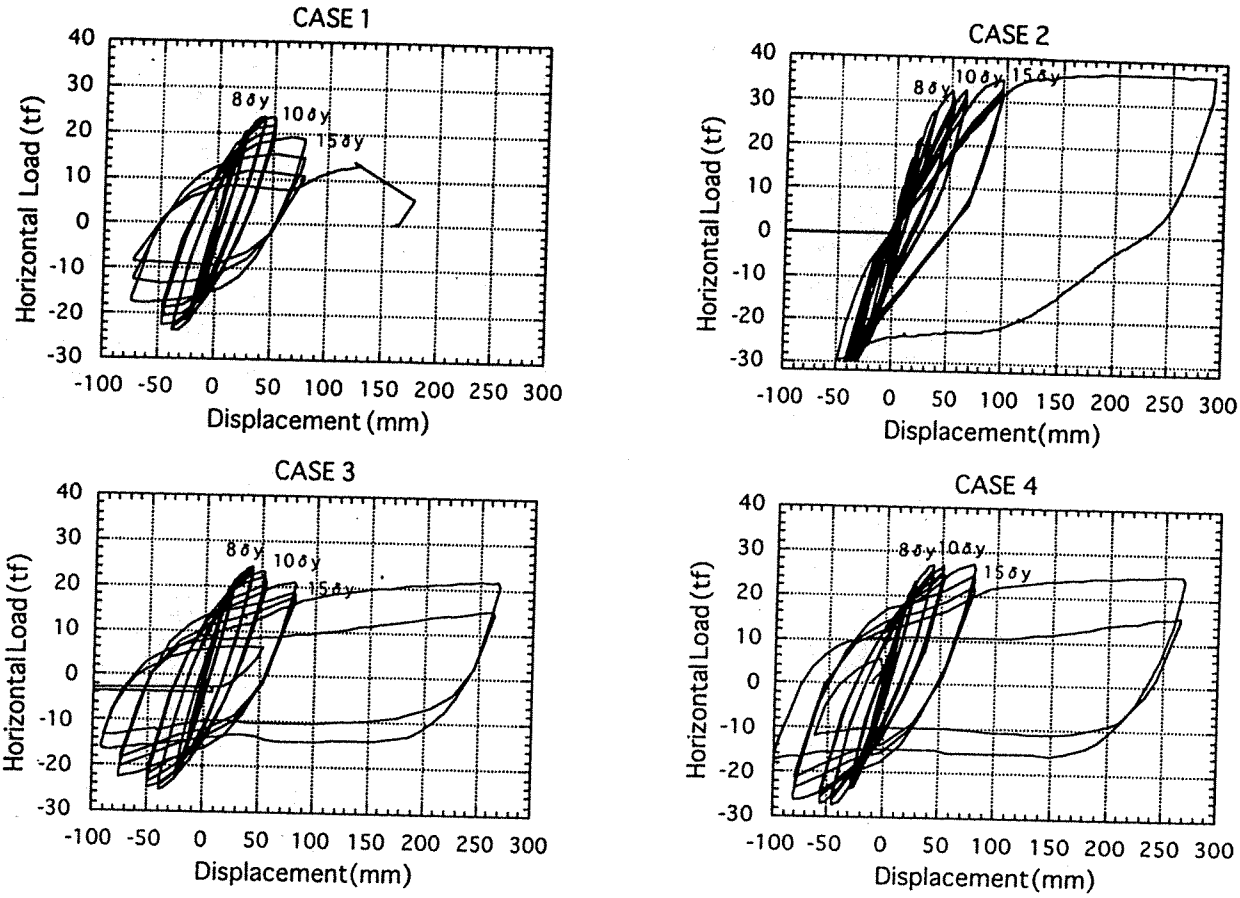

Fig.5 Horizontal Load - Horizontal Displacement Relations

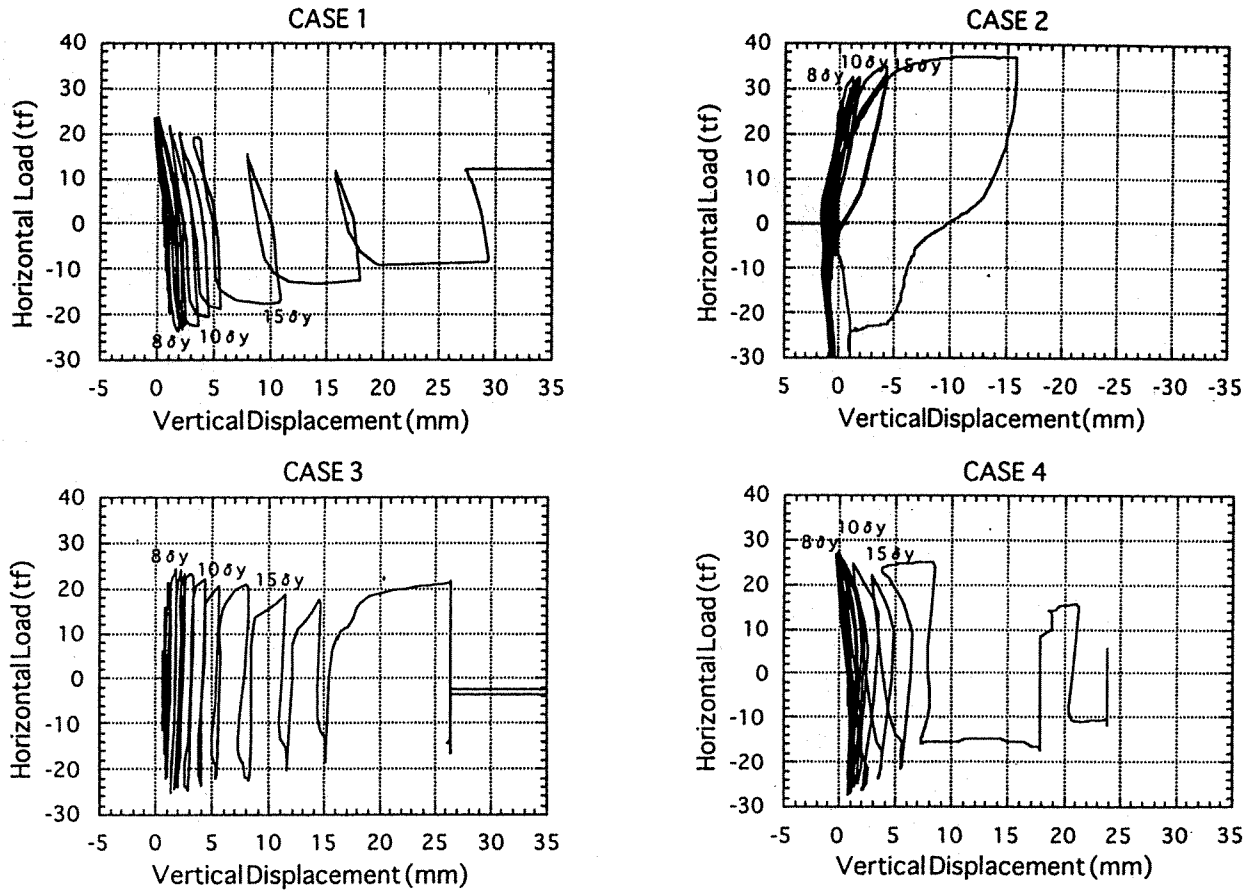

Fig.6 Horizontal Load - Vertical Displacement Relations

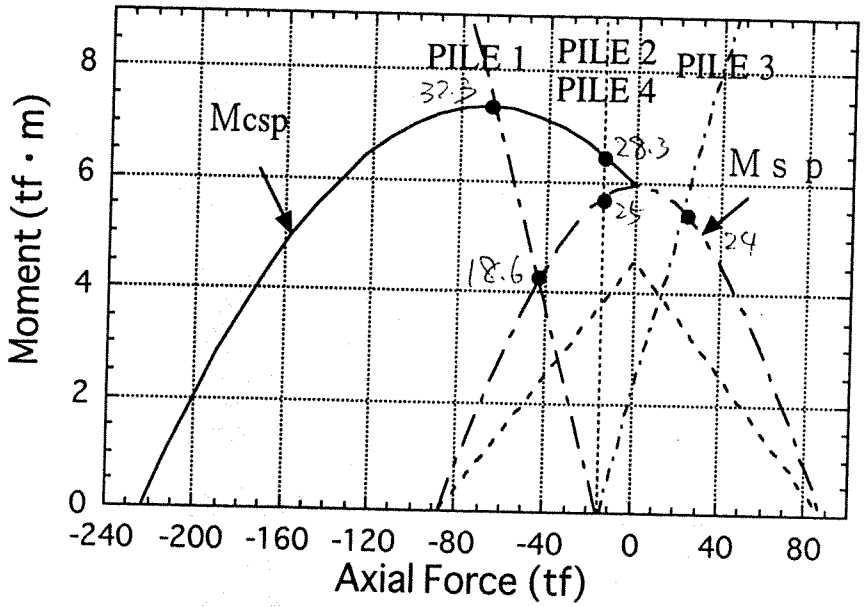

FIg.7 Interaction curves for pipe

Table 1 Measured Maximum Horizontal Load

CASE	Maximum Load
CASE1	23.6 tf
CASE2	37.0 tf
CASE3	23.6 tf
CASE4	27.3 tf

Table 2 Calculated Horizontal Load for the Fully Plastic Moment of Each Pile

	PILE 1	PILE2	PILE3 PILE4
Steel	18.6 tf	25.0 tf	24.0 tf
Steel and Concrete	32.3tf	28.3 tf	24.0 tf

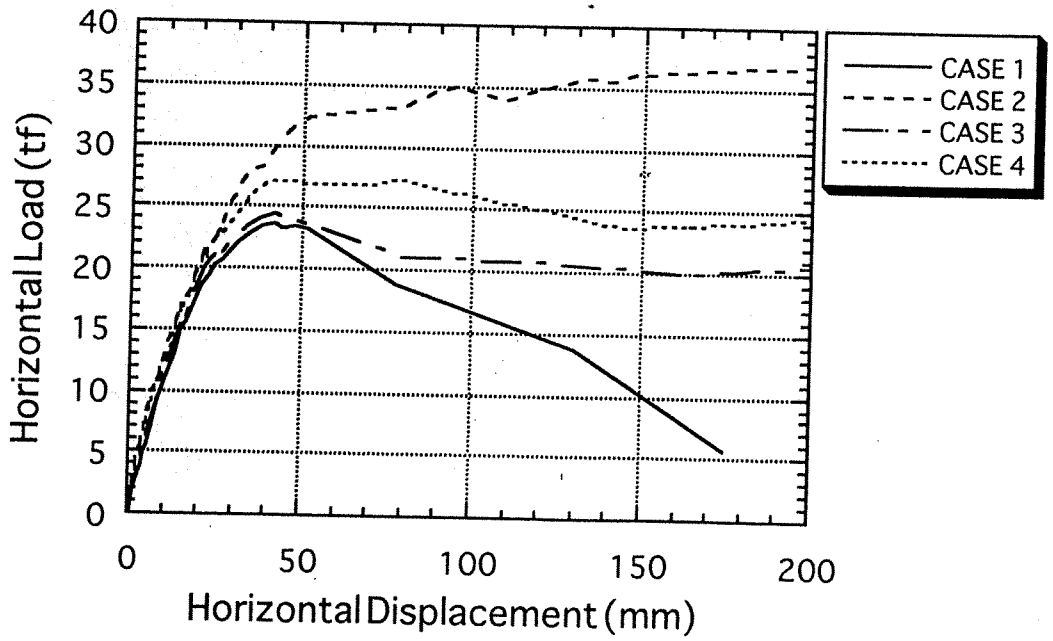

FIg.8 Envelops of Horizontal Load-Displacement Relations

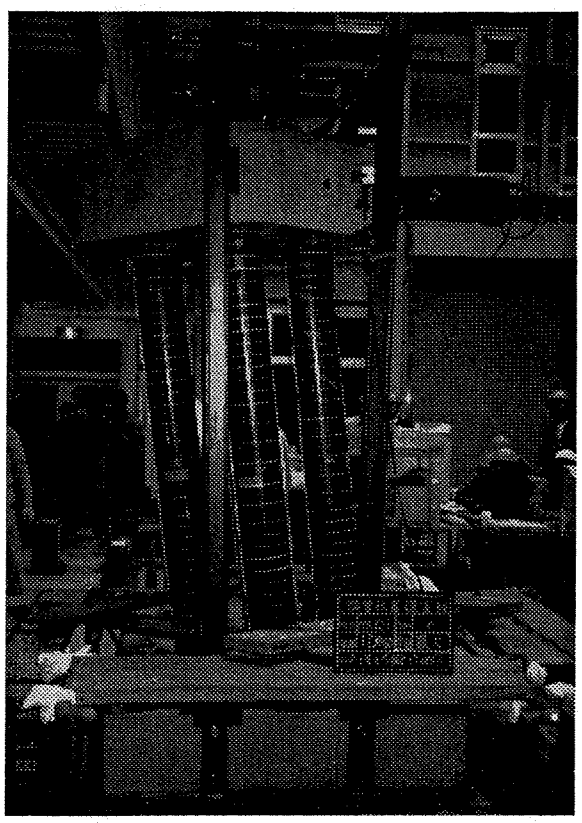

Phot.1 CASE3 at the maximum displacement

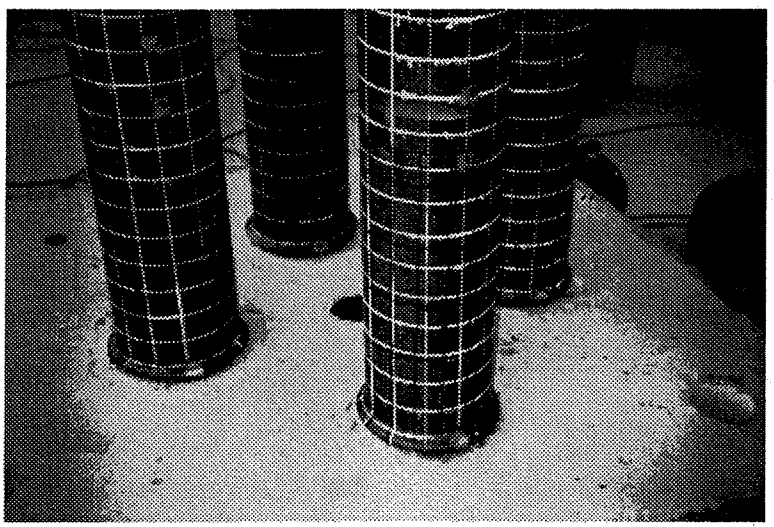

Photo.2 Elephant Foot Buckling (CASE 1)

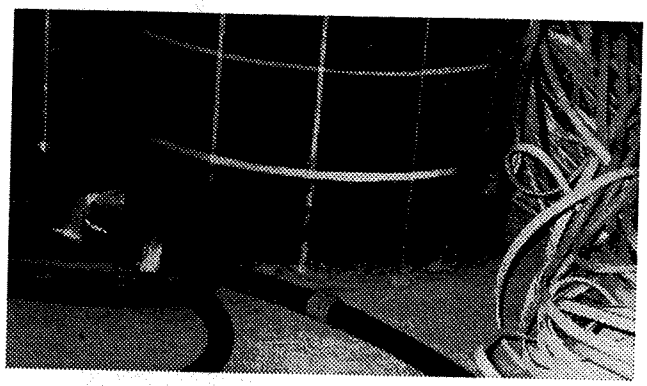

Phot.3(a) End of the Pipe at 8 δ y(CASE 3)

Phot. 3(b) Inelastic Buckling at 15 δ y (CASE 3)

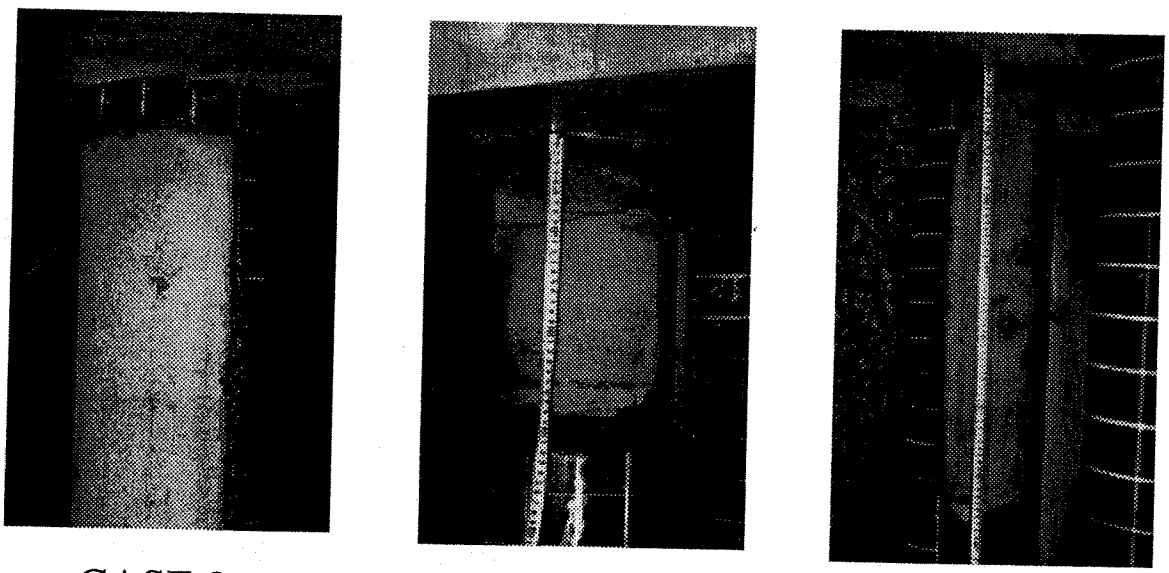

CASE 2 CASE 3 CASE 4

Phot.4 Filled Concrete after the Experiments

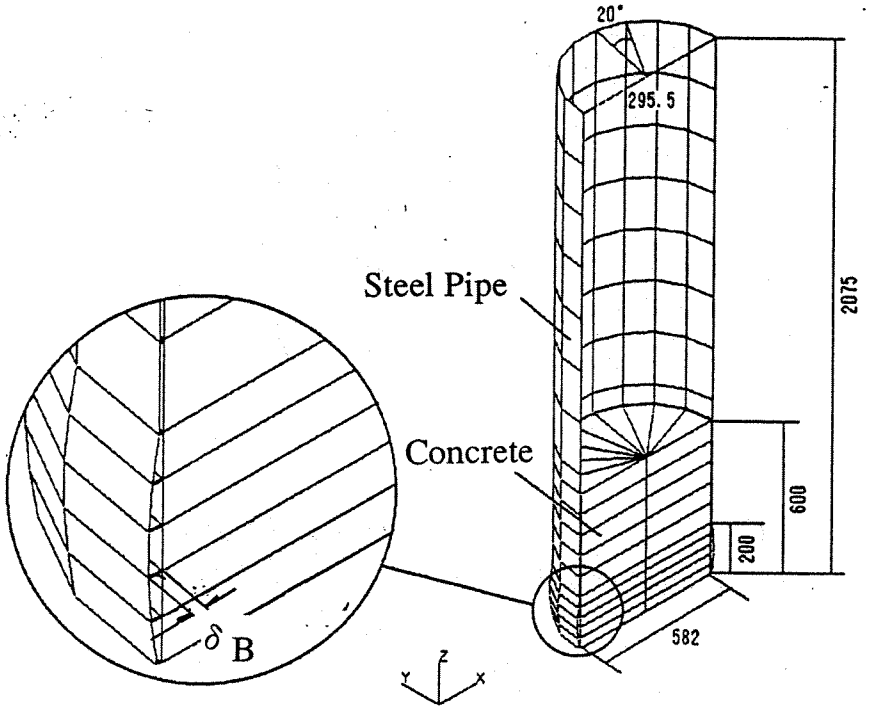

Fig.9 FEM Model

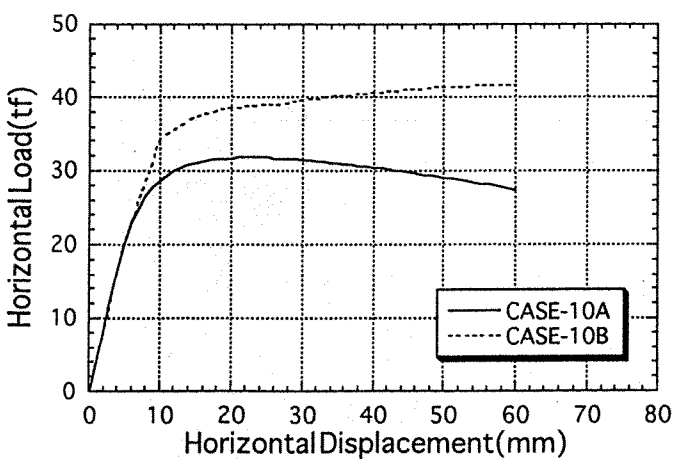

(a) δ_B=10mm

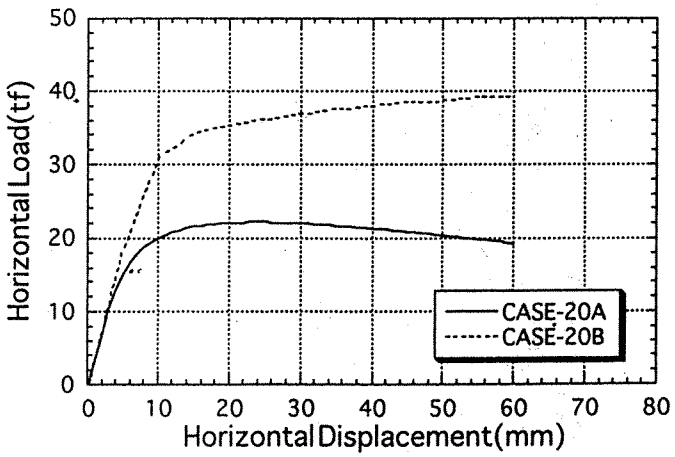

(a) δ_B=20mm

Fig.10 Horizontal Load - Displacements Relations

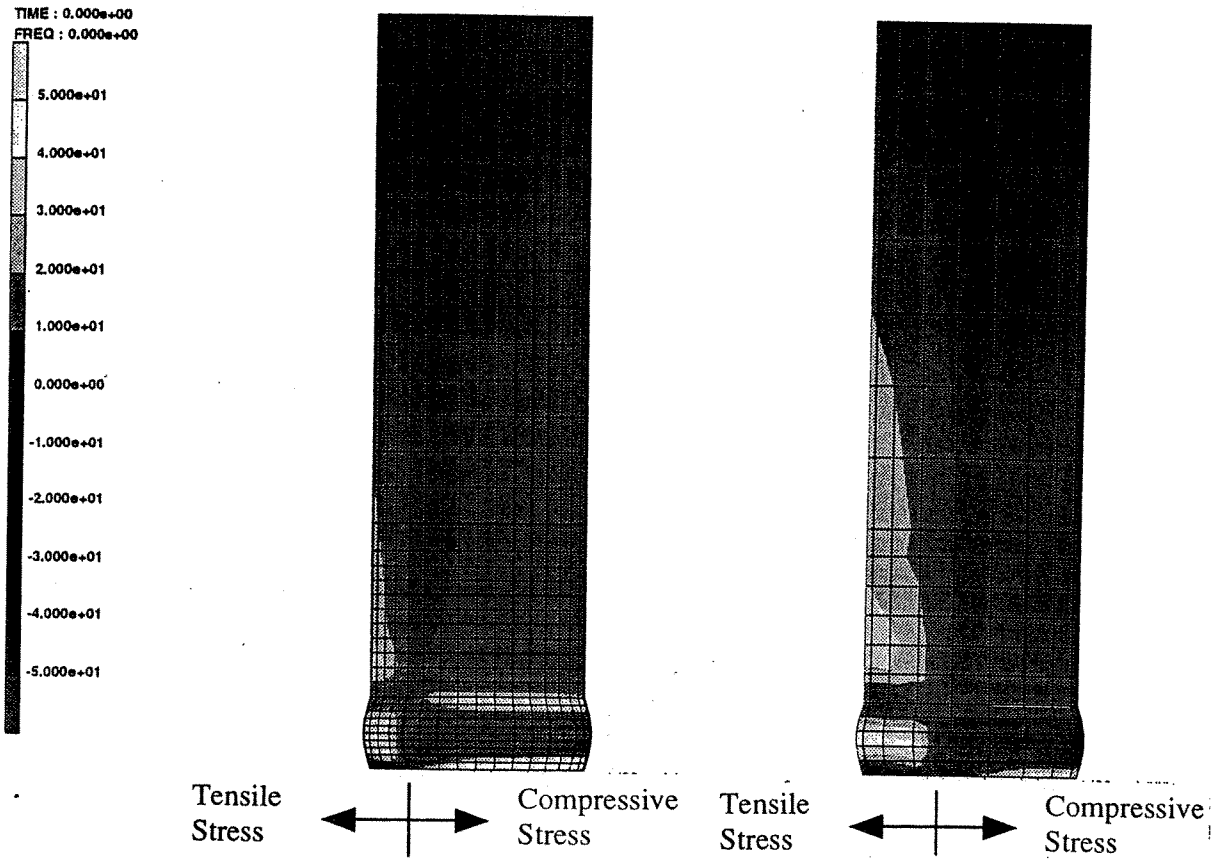

(a)CASE-20A (b)CASE-20B

Fig.11 Distribution of Axial Stress of Steel Pipe

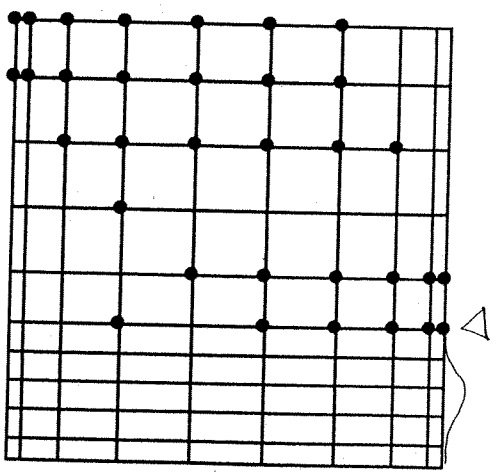

Fig.12 Contact Point between Steel and Concrete (CASE-20B)

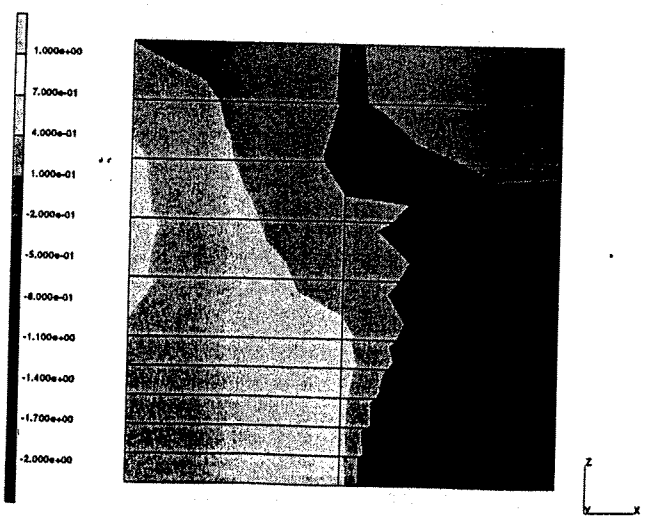

Fig.13 Distribution of Axial Stress of Concrete (CASE-20B)

AN ANALYSIS OF A LANDING PIER OF STEEL PIPE PILES DAMAGED BY 1995 HYOGOKEN-NAMBU EARTHQUAKE

S. Nishizawa[i], M. Hashimoto[i], Y. Sakata[i] and K. Sonoi[ii]

ABSTRACT

Detailed investigation was made on a landing pier of steel pipe piles damaged by 1995 Hyogoken-Nambu Earthquake, and the external force which acted thereon and the mechanism of failure were inferred. Said pier was of an open type supported by vertical and batter piles and was constructed in front of the sea wall caisson. The investigation covered the displacement and inclination of the sea wall and the pier, and buckling and deformation of steel pipe piles were examined after the piles were extracted. In the vicinity of the area near the investigated pier, a horizontal acceleration of 326 gal had been recorded, so a large inertial force may have acted on the sea wall caisson and the pier. In addition, the replacement sand below the caisson may have undergone liquefaction, causing the replacement sand and the rubble to shift and imposing horizontal force directly upon the piles, causing their breakage. Such being the case, in the present analysis a total of eight (8) cases were studied under varying conditions including the

---

[i] Japanese Association for Steel Pipe Piles

[ii] Senior Research Engineer, Nikken Sekkei Ltd.

presence/absence of horizontal force due to ground movement, the loading direction and the magnitude of the horizontal load in addition to the inertial force of the structure generated by the earthquake. As a result, it was found that the case wherein the inertial force of the structure is in the direction opposite to that of the ground deformation load most correctly explained the condition of the damage which actually occurred.

Keywords: pile pier, earthquake damage, port and harbor, liquefaction, site investigation, horizontal load IGC: H7

INTRODUCTION

Detailed investigation was performed on a landing pier of steel pipe piles pier damaged by Hyogoken-Nambu Earthquake (which occurred on January 17, 1995) and the external forces which acted on the steel pipe pile type pier and the mechanism of its failure were estimated. As a result of the analysis performed, it was understood that the cause for the deformation of the steel pipe piles was not only the usual inertia of the structure but also included the effects of the deformation of the rubble of the caisson sea wall behind the pier and the decrease of the shear resistance of the ground under the rubble.

This paper intends to report the results of the investigation of the damage to the steel pipe piles on the site and the results of the analyses made based on said investigation.

OUTLINE OF THE STRUCTURE

The damaged pier in question was constructed in 1969 at Sumiyoshihama-cho, Higashinada-ku, Kobe; it was therefore approximately 25 years old.

The structure of the caisson sea wall behind and the reclamation work was executed during the period from 1963 to 1968.

The outline of the damaged pier is shown below.

① Pier configuration:

The pier was 160 meters long and 12.5 meters wide, the depth of the water in front being 12.5 meters, with the capability to berth a 50,000 DWT vessel. The distance between the sea wall and the pier was 11.7 meters. Fig. 1, Fig. 2 and Fig. 3 show the front view, plan and a typical sectional view of the pier respectively.

② Pier structure:

The structure of the pier is a steel pipe pile type supported by vertical and batter piles (piles in the direction of the face line and batter piles in the direction at right angles to the piles along the face line). The upper structure is of reinforced concrete slab with vertical foundation steel pipe piles of ø558.8 × t9.5 and batter foundation steel pipe piles of ø609.6 x t9.5 and ø711.2 x t9.5. It seems that this pier was designed in accordance with the then effective "Technical Standards for Port and Harbor Facilities" (The Japan Port and Harbor Association) so that the design horizontal seismic coefficient was 0.15.

③ Ground condition:

Fig. 4 shows soil profile at the pier front section taken at the

time of the investigation after the earthquake.

INVESTIGATION

Investigation subjects

It was recognized that due to the earthquake, the north side caisson sea wall had moved seaward and inclined forward. The pier had been damaged with the steel pipe piles buckled and/or deformed, and the pier top inclined landward. Thereafter, all piles of this pier were extracted, and a new pier with an emphasis on earthquake vibration resistance was constructed. The following shows the details of the investigation performed during the process of pile extraction.

① Sea wall: Horizontal displacement of the sea wall, vertical displacement of the top thereof, caisson inclination angle and distance between the sea wall and the pier

② Pier: Horizontal displacement of the pier, vertical displacement of the pier, conditions of damage to the piles (buckling, corrosion) and their inclination angles, deformation of piles after they were extracted

③ Sounding: Sea bottom ground elevation in front of the sea wall and around the pier

The earthquake vibration had deformed not only the pier and the sea wall but also the ground in the entire surrounding area;

therefore, at the time of the investigation datum points such as triangulation station and bench mark were not clear. Such being the case, to put the investigation results in order, assumptions were made so that the site boundary line approximately 100 meters from the sea wall on the land side was considered to be the fixed point, that the elevation of the pier top on the sea side is the same as that before the earthquake and that the base of the driven portion of the steel pipe pile was not displaced. On the other hand, an investigation conducted before the earthquake had confirmed that the sea wall section, before the earthquake, had already suffered consolidation settlement of approximately 80cm.

Investigation results

Major investigation results are shown below, and an example of sea wall-pier-ground deformation diagram estimated based on such investigation results will be shown in Fig. 5.

① Sea wall

- Sea wall face line moved approximately 1.5 - 1.7m seaward.
- Sea wall top settled about 0.6 - 1.0m due to the earthquake. The nearer a portion was to the pier central section, the smaller the settlement was.
- Sea wall caisson as a whole inclined 3 - 4° seaward.

② Pier

- Pier face line moved about 10 - 60cm toward the sea wall.
- Pier top inclined approximately 1/20 - 1/40 toward the sea wall. The nearer a portion was to the pier central section,

the larger the inclination was.

- Steel pipe piles were bent near the foot protection stone. The nearer the pile was to the sea wall, the larger its deformation (max. approx. 100cm; see Photo 1).

③ Sea bottom ground

- Sea bottom ground configuration before the earthquake is unknown; the result of the sounding shows that, compared with the configuration shown in the typical section drawings, the rubble under the caisson foot had bulged forward.

In the vicinity of the Higashi-Kobe Ohashi Bridge approximately 2km from the pier, a horizontal acceleration in the north-south direction of 326 gal and a vertical acceleration of 396 gal at the ground surface were record[1]. In addition, the ground around the pier structure site, which is a reclaimed area, had suffered liquefaction all over, and sand spouts and ground subsidences were also observed near the sea wall. These phenomena lead to the assumption that a large inertial force due to the earthquake acted upon the caisson pier, and the replacement sand under the caisson was affected by liquefaction. Further, it seems that the rubble and replacement sand under the caisson moved forward to apply horizontal force upon the piles; this is assumed from the fact that the caisson moved about 1.5 - 1.7m seaward, that the rubble under the caisson bulged and moved forward and that the piles were bent seaward near the sea bottom ground surface.

ANALYSIS

Conditions for analysis

With the use of the analysis system "Super DYNAMICS", which is capable of handling elastoplastic behaviors of 3-dimensional structures, the inertial force of the structure and the external force due by the ground deformation were applied gradually as static loads.

Ground deformation is considered to be attributable to the decrease of shear resistance of the replacement sand. Therefore, the cases where the ordinary design method is used assuming the sea bottom does not deform (MODEL-A) and other cases where the sea bottom ground deformation effect is considered (MODEL-B) were analyzed separately. A total of eight (8) cases as shown in Table 1 were analyzed.

In the cases of MODEL-A, the acting load was limited to the inertial force of the structure, the acting direction being from land to sea in CASE-1 and the reverse acting direction in CASE-2. In the cases of MODEL-B, the ground spring of the rubble and the replacement sand was not provided, and in all cases the ground deformation load was applied. In CASE-3 only the ground deformation load was imposed; in CASE-4 the structural inertial force from land to sea was applied in addition to the ground deformation load; and in CASE-5 the structural inertial force was appositely applied from sea to land. In CASE-6, CASE-7 and CASE-8, the ground deformation loads were assumed to be half of those applied in CASE-3, CASE-4 and CASE-5 respectively.

Analytical models

(1) Structural models

For structural models, materials were assumed as shown below, and, as shown in Fig. 6, the pier was transformed into 2-dimensional plane models for the purpose of analysis.

- RC upper structure --- Elastic bending member
- Steel pipe pile --- Elastoplastic bending member (Yield judgment possible every 1m)
- Ground --- Elastoplastic spring

(2) Ground spring constant

Coefficient of horizontal subgrade reaction for each ground layer was converted based on N-value[2] so that the maximum value of ground resistance was assumed to be the passive earth pressure strength of the ground. For the coefficient of horizontal subgrade reaction of batter piles, correction was performed using the method proposed by Kubo, et al.[3] The coefficient of vertical subgrade reaction of the pile tip and the vertical shear ground reaction force coefficient of the pile circumferential surface were calculated assuming the open end pile driven steel pipe pile[4], and the pile ultimate bearing capacity and ultimate extraction force (driven piles) were taken as the maximum value of pile tip resistance.

(3) Load

As to the loads on the steel pipe pile, the RC upper structure

dead load and the steel pipe dead load were included as vertical load, and the RC upper structure inertial force under earthquake and the horizontal force due to ground movement were included as horizontal force.

Further, it was presumed that the load from ground deformation was caused by the movement of the rubble and the foot protection stone within a certain area. The actual scope of ground movement could not be specified so it was presumed that under the pier the rubble and the foot protection stone moved as a whole, and behind the pier, an approximately 2m thick rubble layer between the pier and the sea wall moved as a whole. Further, it was assumed that the magnitude of the horizontal force attributable to such movement is proportional to the seismic intensity. Furthermore, judging from the ground movement direction and the steel pipe pile disturbance, piles on the sea wall side are thought to have received more horizontal force. Accordingly, it was assumed that for each pile, depending on its layout position, shear and horizontal force caused by the movement of the rubble and the foot protection stone layer were as shown in Fig. 7.

As to the load application method, all vertical loads were applied at one time as the initial condition, and an external force in the form of a horizontal load corresponding to an increment for horizontal seismic coefficient of 0.01 - 0.05 was applied step by step.

4-3 Analysis results

In the case of CASE-1 and CASE-2 wherein only the structural inertial force was applied, the axial force on batter piles increased as the seismic intensity increased, and first the batter pile head on the compression side yielded and then the section near the sea bottom ground surface yielded. In this yield mode, the axial force is dominant compared with the bending moment. Thereafter, the condition changes as if only vertical piles are exist; therefore, the bending moment of the vertical pile head section increases until it yields in a final failure pattern. Accordingly, the static condition of the pile as bent cannot be explained. The horizontal displacement of the pier top corresponding to the recorded acceleration of 326 gal near the pier structure site was less than 10cm, which is less than the measured displacement.

In CASE-3 and CASE-6 wherein the only ground deformation load was imposed on the pile foot protection stone, the bending moment and the horizontal displacement at the load application point increased as the seismic intensity increased; yielding started at the load application point and then pile head yielding followed. However, the pier top was moved seaward so that the actual failure mode cannot be explained.

In CASE-4 and CASE-7 the structure inertial force was applied in the same direction as that of the ground deformation load. In these cases, however, the pier top moves seaward; therefore, such behavior shown is different to the actual condition which took

place.

In CASE-5 and CASE-8, the structural inertial force was given in the direction opposite to that of the ground deformation load. In these cases, the change in the axial force is small as the horizontal forces are offset. Pile No. 2 and Pile No. 6, on which a relatively large ground deformation load was applied, reached yielding conditions at three (3) points, namely the pile head, the loaded point and the underground section, as the load increased. Because of this, the displacement development during horizontal load increase was large. In CASE-8 in particular, Pile No. 2 was bent seaward coinciding with the mode of damage which actually took place. In the meantime, Pile No. 2 and Pile No. 6 yielded under compression so that the pier top must incline landward more than the analysis result, and this also tends to agree with the phenomenon which actually took place. Moreover, the act that the development of the deformation becomes faster at about a horizontal seismic coefficient Kh of 0.3 is also in good agreement with the actual phenomenon.

Of the eight (8) cases of analysis, CASE-8 most resembled the actual damage condition of the pier. In comparison with CASE-2, wherein the effect of ground movement was not considered, the displacement diagrams and the bending moment of the piles of both cases are shown in Fig. 8, and the transition of the pile tip axial forces are shown in Fig. 9.

Estimation of the pier failure mechanism

(1) Pier strength estimation

This pier had been designed by the allowable stress method to withstand an external force of a horizontal seismic coefficient of Kh = 0.15. However, according to the analysis results of CASE-2, wherein the structural inertial force alone is increased, when kh = 0.30 or so, the pile extraction force reaches its maximum, as can be seen from Fig. 8 and Fig. 9, but the pier is still not close to such condition as failure. The pile head at last reaches the yield point when approximately Kh = 0.40 is reached.

Therefore, if the loading condition is as considered at the time of design, in other words only the structural inertial force is applied, the batter steel pipe pile combined pier could possibly maintained a structurally stable state in general against the horizontal acceleration at 326 gal which was recorded in the vicinity of the pier structure site.

(2) Estimation of the load which acted upon the pier

The results of the pier deformation analysis show that the loading condition of CASE-8, wherein the structural inertial force is applied in the landward direction which is opposite to the direction of the ground deformation load from the sea wall to the sea, is able to explain the actual damage condition of the pier well. In other words, CASE-8 generally reproduced the actual condition of damage including the horizontal displacement toward the sea wall and the inclination toward the sea wall of the pier top, the bending of the steel pipe

piles near the sea bottom ground surface, etc.

It is added that the results of the 2-dimensional effective stress dynamic analysis of the caisson sea wall performed by the Ministry of Transport[5] shows that the conditions of the movement toward the sea wall front of the replacement sand layer including the rubble mound due to the late earthquake are well simulated.

All things considered, it is presumed that the damage to the pier this time was caused by the action of a ground deformation load which was not taken into consideration at time of design in addition to the structural inertial force.

(3) Presumption of the sea wall-pier-ground behaviors and the pier failure mechanism

Based on the results of the investigation and the analyses described above, the mechanism of the pier failure which occurred this time was estimated as follows.

① Earthquake vibration raised the excessive pore water pressure in the replacement sand layer portion, reducing the shear resistance (see Fig. 10 ①).

② At the time of the earthquake, the inertial force and the earth pressure forced the caisson to move forward, simultaneously generating its sinking into the replacement sand layer (Fig. 10 ②).

③ Ground consisting of replacement sand including the rubble mound moved forward (Fig. 10 ③).

④ Horizontal force due to the ground movement acted on the sea bottom portion of the steel pipe piles on the sea wall side (Fig. 10 ④).

⑤ Due to the action of the inertial force (toward the sea wall) of the upper structure generated at the time of the earthquake, the steel pipe pile yielded at three (3) points, namely the pile head section, near the sea bottom ground surface and underground (near the stratum formation interchange point) (Fig. 10 ⑤).

⑥ Due to the action of the compressive force on the sea wall side steel pipe piles, the piles buckled; simultaneously, horizontal displacement developed and the pier top inclined toward the sea wall (Fig. 10 ⑥).

⑦ Due to the resistance decrease of the sea wall side piles, the ground deformation load was transferred to the sea side piles (Fig. 10 ⑦).

⑧ The area in which the sea side steel pipe piles were yielding expanded as the failure of the pier progressed (Fig. 10 ⑧).

CONCLUSIONS

In the present study, a load due to ground deformation was tentatively provided for simulation of the behaviors of the pier; however, it is presumed that what matters essentially is the external force which has relation to the seismic intensity and the resultant sea wall and replacement sand layer subsidence, the horizontal displacement, the distance between the sea wall and the pier, the pile layout, etc.

It is expected that said external force can be clarified and established through numerical analyses such as FLIP, FLAC, etc., which are capable of analyzing large displacement analyses, or through research using centrifugal model experiments, etc.

The results of the study made this time help us understand that the failure of the subject pier by the earthquake was largely affected by the damage of the sea wall in the back, considering the fact that the quays of Port Island and Rokko Island moved 4 - 5m forward and that the cargo unloading quay in the Kakogawa area moved 10 - 15m. This suggests that to maintain stability at time of an earthquake of a pier constructed in front of a sea wall, the seismic resistance of the pier itself must be secured and that in addition, the stability of the sea wall in the back has an important relationship.

Further, it was understood that depending on the pier position, a horizontal load due to the displacement of the ground at the sea wall section acts on the piles of the pier. In this case, not only the pier support function but also a substantial the sea wall deformation prevention function is expected to the piles structures. Therefore, it is necessary to review the structure itself of the steel pipe piles in addition to its bearing force mechanism and yield strength.

Therefore, it could be said the impending requirements in planning a pier structure near a sea wall from now on are to develop a method which is capable of properly evaluating the sea wall stability under seismic motion and the effects of the related overall ground deformation, and further, to develop a sea wall structure resistant to earthquakes, whether for new structure or for reinforcement of existing sea walls.

REFERENCE

1) Interim Report of Investigation on Damage to Evaluated Roads Inflicted by 1995 Hyogoken-Nambu Earthquake, Mar. 1995, Elevated Road Earthquake Damage Countermeasure Committee in Hyogoken-Nambu Earthquake

2) Technical Standards for Port and Harbor Facilities and Explanation, 1989, The Japan Port and Harbor Association

3) Experimental Research on Lateral Resistance of Piles (Part 3), Koichi Kubo, Port and Harbor Research Institute Report, Vol. 12, No. 2, March. 1962

4) National Railways Structure Design Standard Explanations, 1985, Japan Society of Civil Engineers

5) Port and Harbor Engineers Seminar Text on Earthquake Damage Countermeasures, Oct. 1995, Coastal Development Institute of Technology

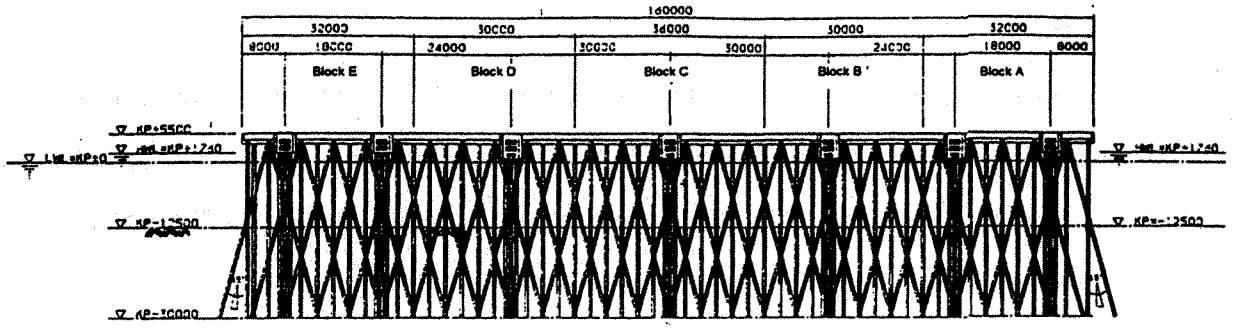

Fig. 1 Front view of the pier

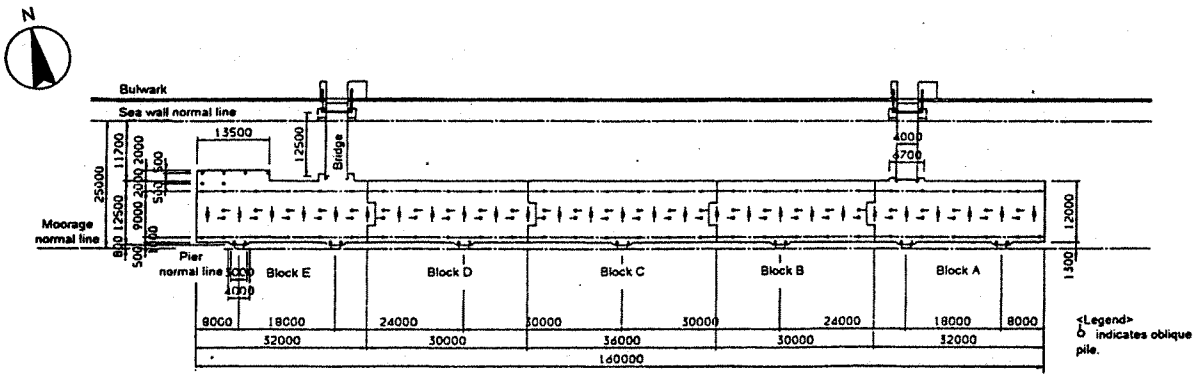

Fig. 2 Plan of the pier

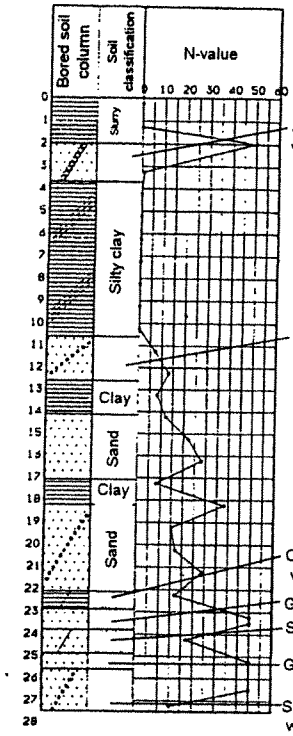

Fig. 4 Soil profile

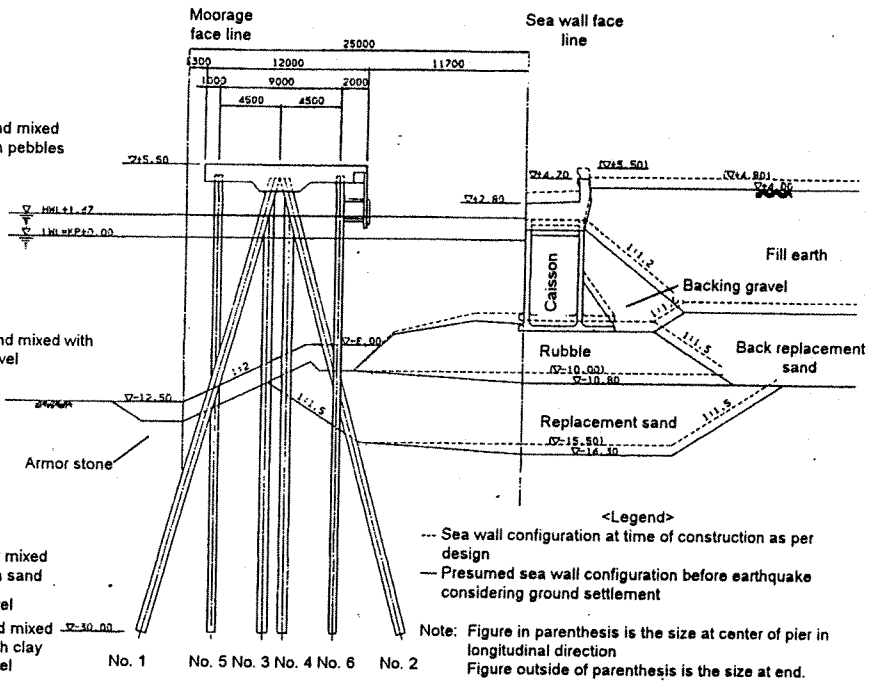

Fig. 3 Typical section of pier

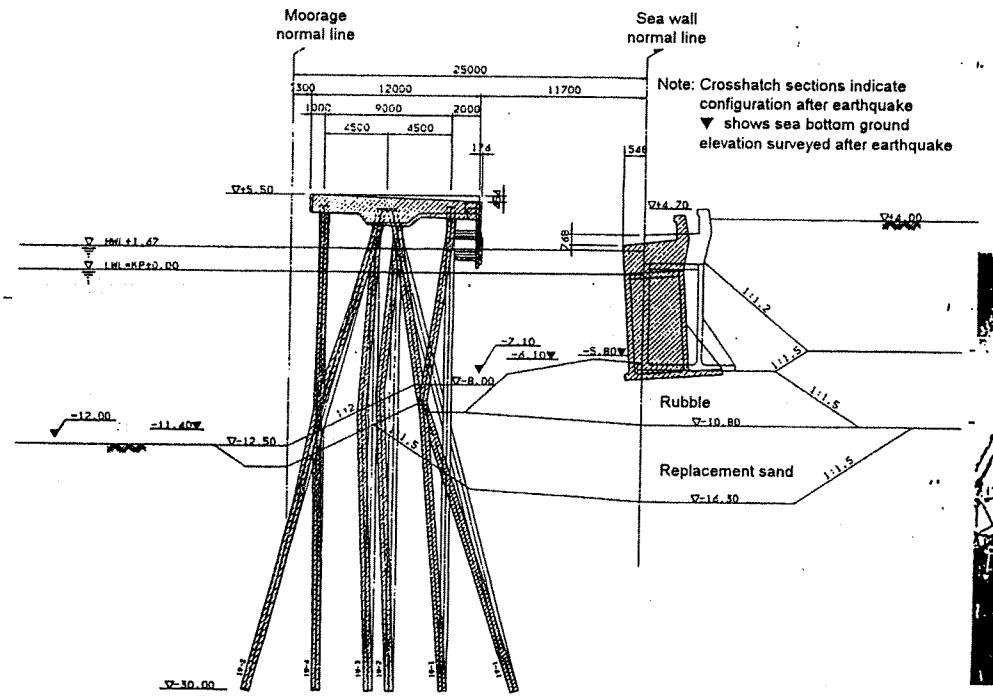

Fig. 5 Deformation after earthquake

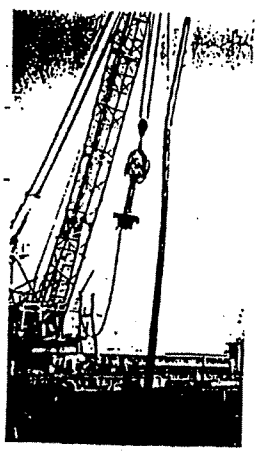

Photo 1 Pile as deformed

Table 1 List of analysis cases

		Ground behavior	
		Dormant	Active
Analysis model (Direction of action)		MODEL-A	MODEL-B
Horizontal load	Structural inertial force (Sea ← Land)	CASE-1	-
	Structural inertial force (Sea → Land)	CASE-2	-
	Ground deformation load (Sea ← Land)	-	CASE-3' (CASE-6)
	Structural inertial force (Sea ← Land) + Ground deformation load (Sea ← Land)	-	CASE-4 (CASE-7)
	Structural inertial force (Sea → Land) + Ground deformation load (Sea ← Land)	-	CASE-5 (CASE-8)

Note: Horizontal ground spring of the batter piles at right angles to the normal line in CASE-1 and that in CASE-2 are replaced.

Note: Evaluated ground deformation loads of CASE-3, -4 and -5 are halved in CASE-6, -7 and -8.

	N-value	ø°	γ' kN/m³	γ' kN/m³
Rubble	40	40	17.64	9.8
Pile base foundation stones	40	40	17.64	9.8
Replacement sand	15	30	17.64	9.8

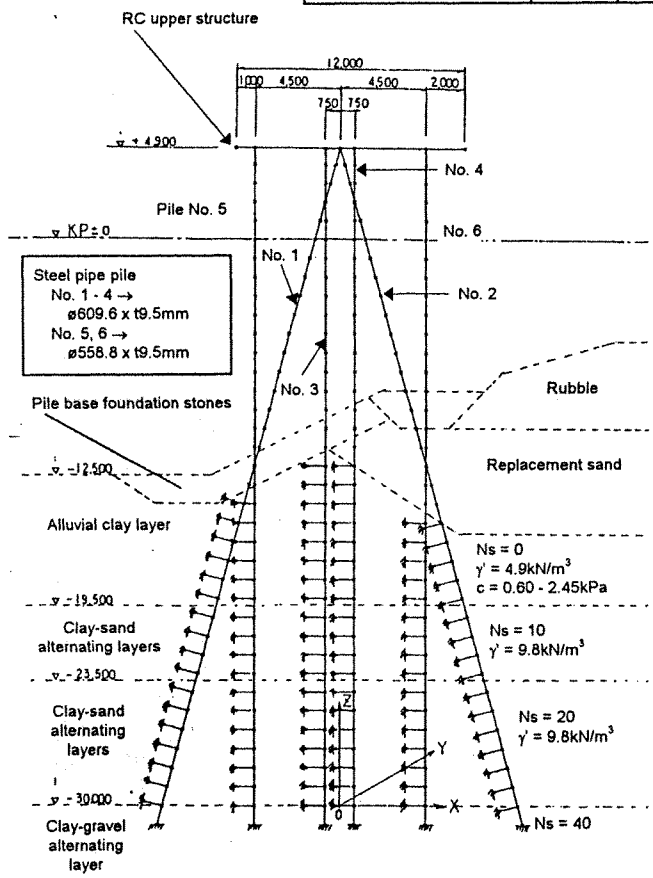

Fig. 6 Model formation and ground conditions

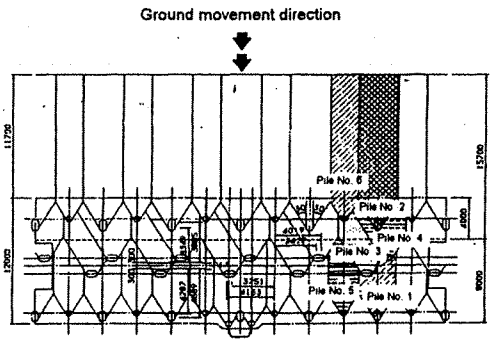

Fig. 7 Areas of horizontal forces shared by respective piles S= 1:200

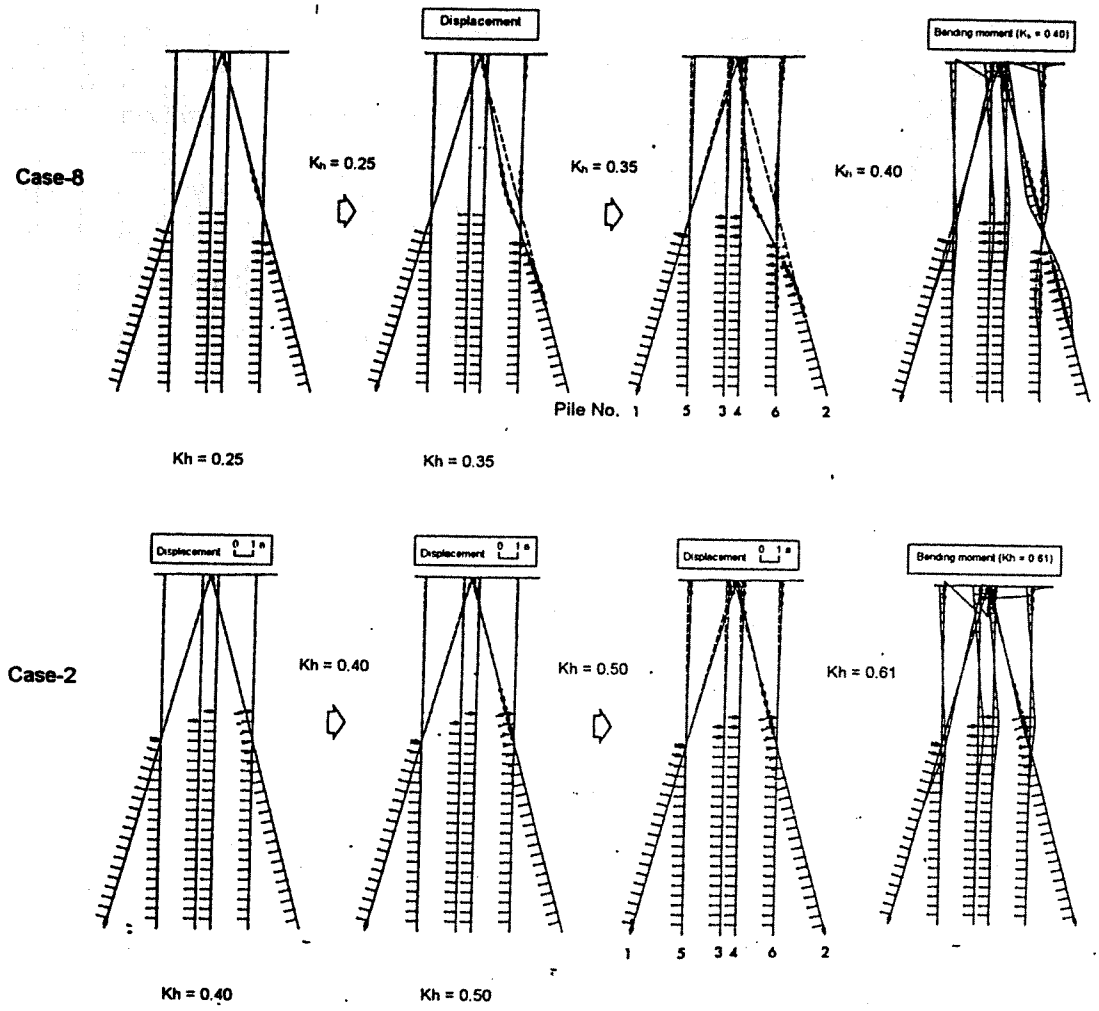

Fig. 8 Case - 8/2 analysis results

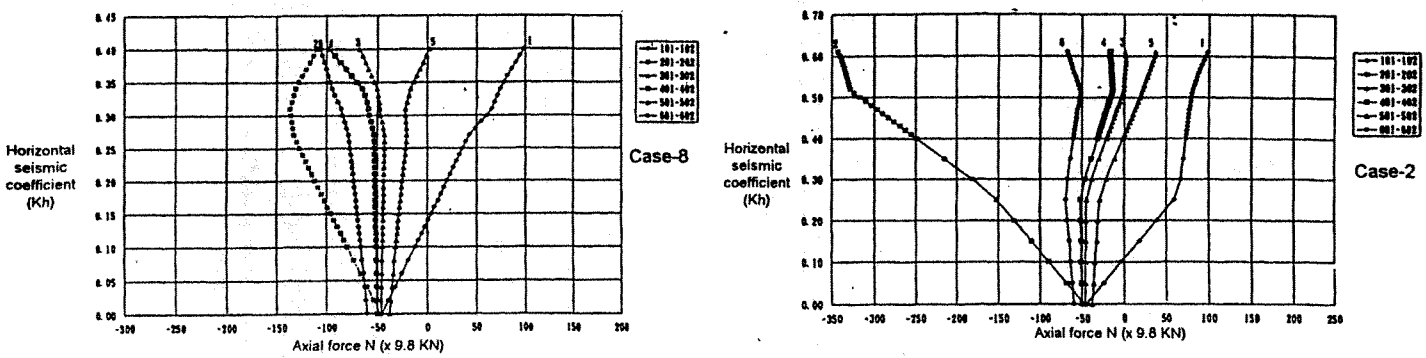

* Figures in the diagram represent pile numbers.

Fig. 9 Axial force transition of pile tip (CASE-9)

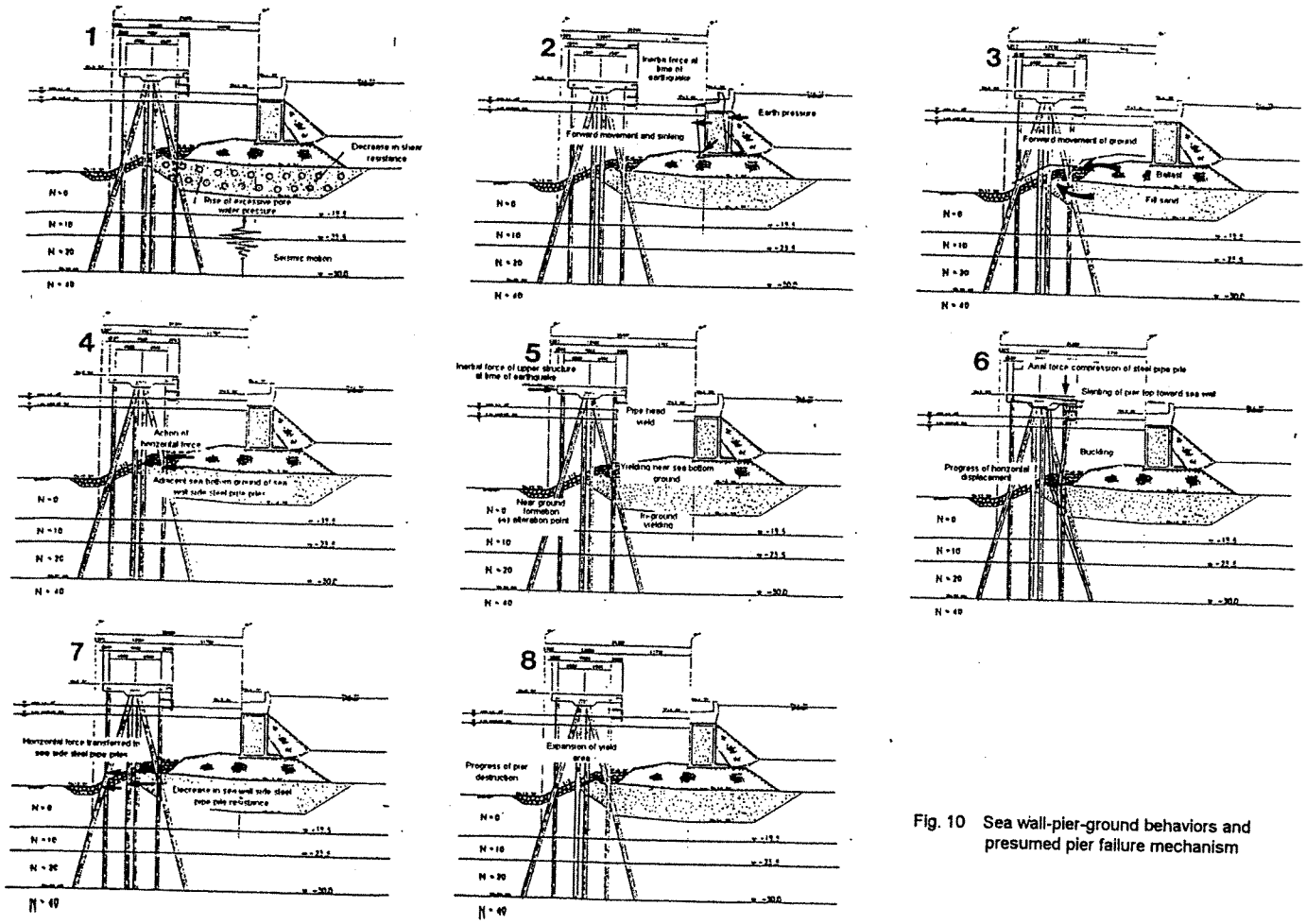

Fig. 10 Sea wall-pier-ground behaviors and presumed pier failure mechanism